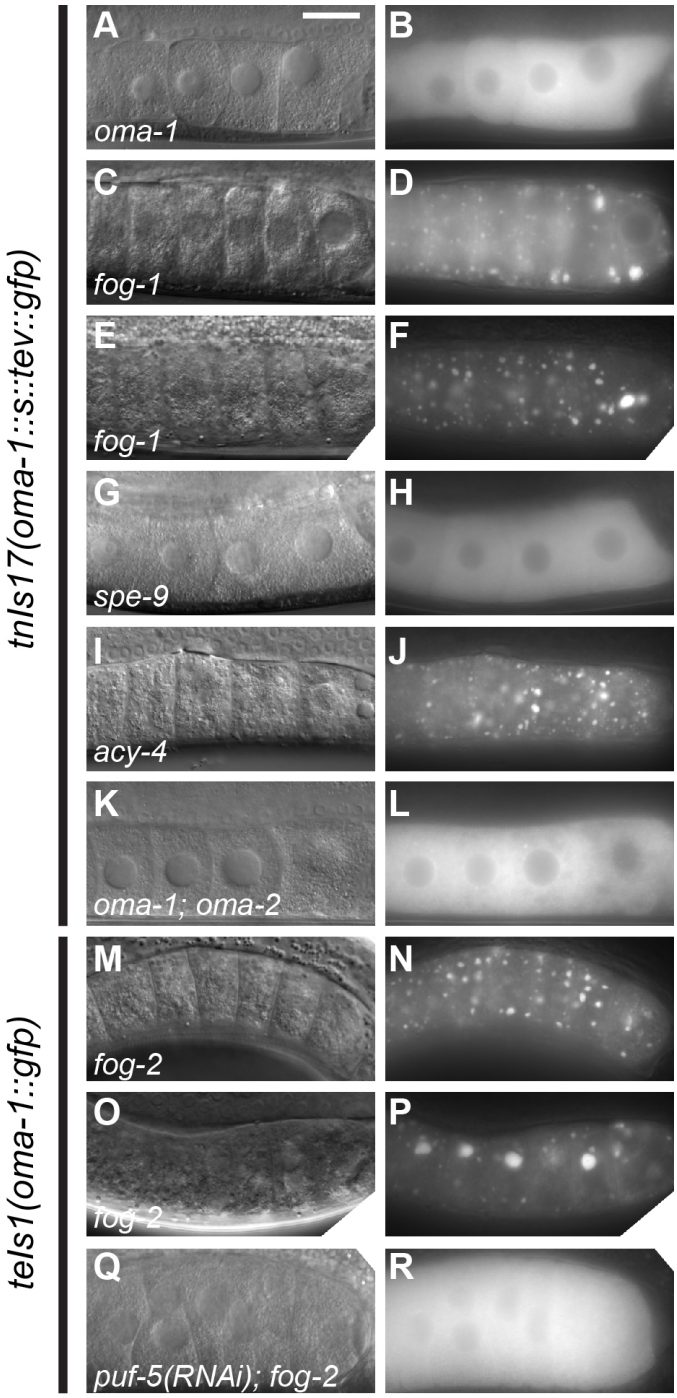

Figure S1 OMA-1 reorganizes into large RNPs when sperm-dependent signaling is compromised. GFP-tagged OMA-1 aggregate when sperm are absent (D, F, N, P) or adenylate cyclase (*acy-4*) signaling in gonadal sheath cells is abrogated (J). Aggregation of OMA-1::GFP in the absence of sperm requires PUF-5 (R) and CAR-1 (C. Spike, unpublished results). OMA-1::GFP aggregates are most easily visualized in surface focal planes (F, J, N, P), but can also be seen in medial focal planes (D) where diffuse OMA-1::GFP is most easily visualized (B, H, L, R). DIC and GFP images of oocytes are on the right and left, respectively. Genotypes: *unc-119(ed3)*; *oma-1(zu405te33)*; *tnIs17[oma-1::s::tev::gfp, unc-119(+)]* (A, B); *fog-1(q253*ts*); oma-1; tnIs17* at 25°C; (C–F) *spe-9(hc88*ts*); oma-1; tnIs17* at 25°C; (G, H) *acy-4(ok1806) tnIs17* (I, J); *oma-1; oma-2(te51) tnIs17* (K, L); *fog-2(q71); teIs1[oma-1::gfp, unc-119(+)]* (M–P); *puf-5(RNAi); fog-2(q71); teIs1* (Q, R). Bar, 20 µm.

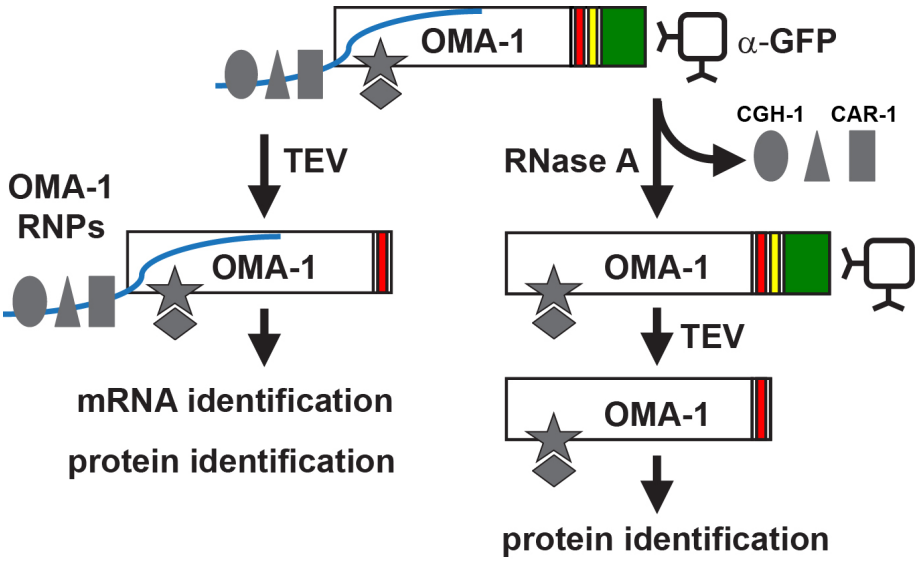

Figure S2 Purification strategies used to characterize OMA-1-interacting mRNAs (left) and proteins (right). OMA-1 was tagged with an S-tag (red), tobacco etch virus (TEV) protease cleavage site (yellow) and GFP (green). Tagged OMA-1 is immunopurified using anti-GFP antibodies and eluted from the immunoaffinity matrix by digestion with TEV protease, releasing mRNA (blue) and protein (gray) components of OMA-1 RNPs. RNase A treatment of immunopurified OMA-1 releases many RNP-associated proteins, including CGH-1 and CAR-1. Proteins that are closely associated with OMA-1 are eluted from the immunoaffinity matrix after RNAse treatment by digestion with TEV protease. These proteins either interact with OMA-1 through protein-protein interactions (shown), or have an RNA-dependent interaction with OMA-1 that is resistant to RNase treatment. Our RNase treatment method was clearly effective because many proteins were eluted by RNase treatment (Figure 1C) and no CGH-1 peptides were recovered following RNase treatment (File S2).

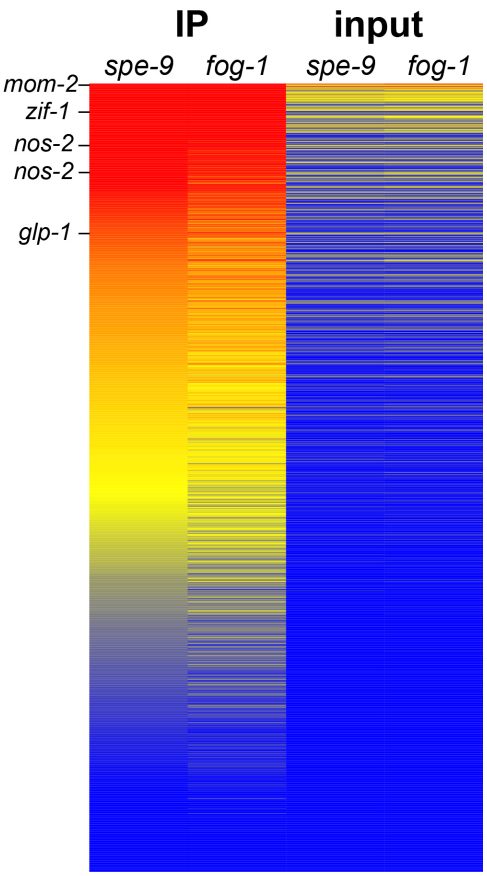

Figure S3 Previously identified mRNA targets of OMA-dependent translational repression appear to be abundant in OMA-1 purifications. The average raw intensity values of probe sets up at least 2-fold in OMA-1 purifications (*P(corr)* $\leq$ .05) in the presence and absence of MSP-dependent signaling (*spe-9* and *fog-1* genotypes, respectively) are illustrated. Higher intensity values are in red (values $\geq$ 90th percentile in the *fog-1* purifications), mid-range values are in yellow (50th percentile), and low intensity values are in blue ($\leq$10th percentile). The probe sets detecting *mom-2*, *zif-1*, *nos-2*, and *glp-1* all have high-intensity values in OMA-1 purifications (IP) and lower-intensity values in the input samples, which are shown for reference. Probe sets are ranked from high to low using the intensity values in the first column (*spe-9* purifications).

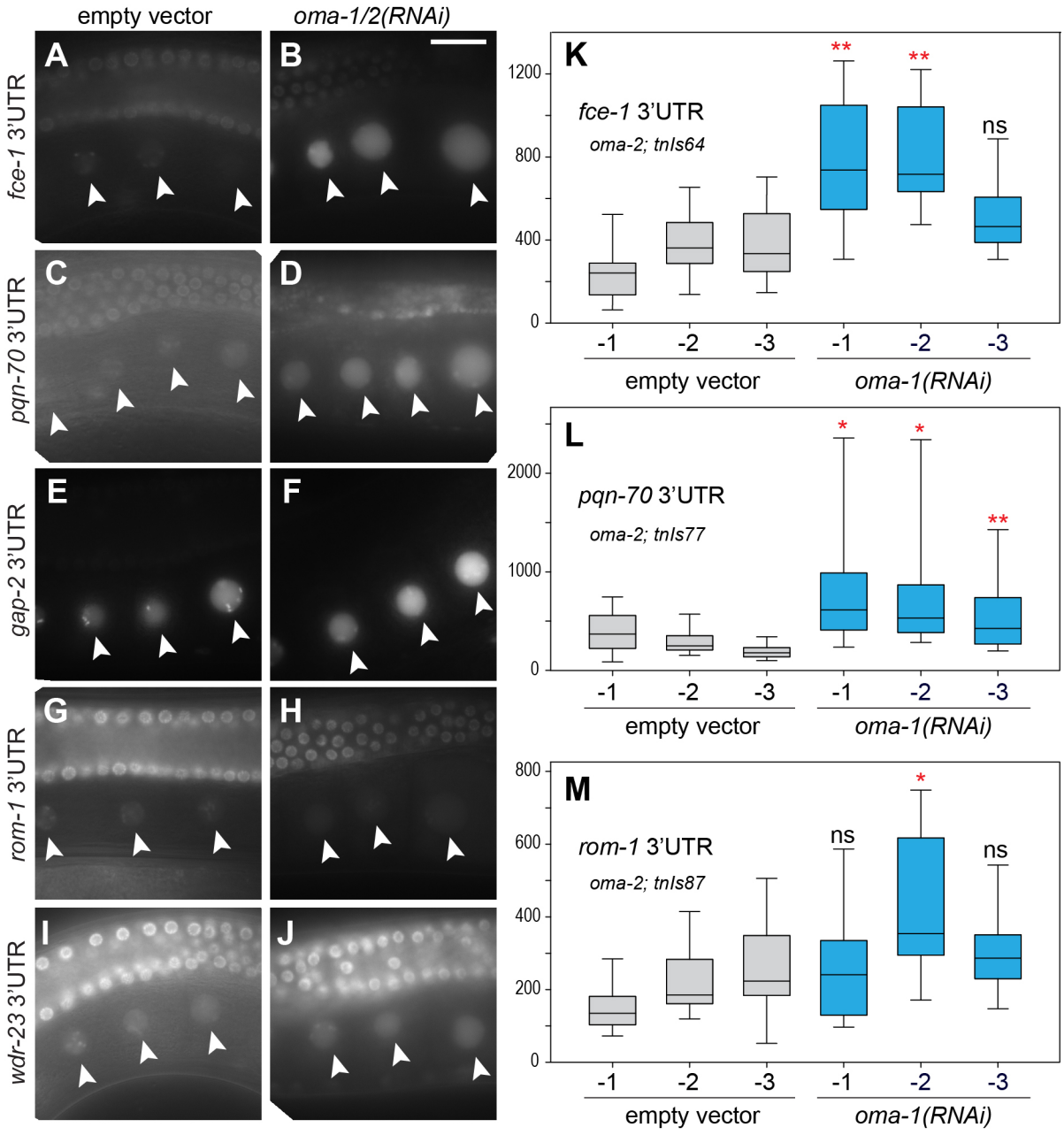

Figure S4 OMA-1-associated 3'UTRs that are weakly repressed or not regulated by OMA-1/2. GFP::Histone 2B (H2B) expression from a reporter transgene containing either the *fce-1* (A, B, K), *pqn-70* (C, D, L) or *gap-2* (E, F) 3' UTR is modestly increased in oocytes after reducing *oma-1/2* function. GFP::H2B expression from a reporter transgene containing either the *rom-1* (G, H, M) or *wdr-23* (I, J) 3'UTR is unaffected. *oma-1/2* function was compromised using *oma-1/2(RNAi)* (B, D, F, H, J) or by combining *oma-1(RNAi)* with a loss-of-function mutation in *oma-2* (K–M). Background-corrected nuclear GFP intensity (in arbitrary fluorescence units, plotted on the y-axis) was measured for the three oocytes closest to the spermatheca (x axis, oocytes –1 to –3) and is significantly increased in *oma-1/2* oocytes as indicated (two asterisks, $P \leq 0.001$; one asterisk, $P < 0.05$; ns, not significant, using the Mann-Whitney U-test). Box plots represent the data from 10 oocytes in each position. Box plot whiskers indicate the minimum and maximum background-corrected intensity values. Bar, 20 µm.

A

Construct 3'UTR	Distal	Pachytene	Loop	Oocytes	Early Embryos
zif-1	++	+	-	-	+
cdc-25.3	++	++	+	+/-	+
rnp-1	++	++	+/-	+/-	+
rnf-5	++	++	+	+	-
fce-1	++	++	+	+	-
pqn-70	++	++	++	++	+
gap-2	+	+	+	++	-
wdr-23	+	++	+	+	-
rom-1	+	++	+	+	-
fbf-2	++	+/-	-	-	-

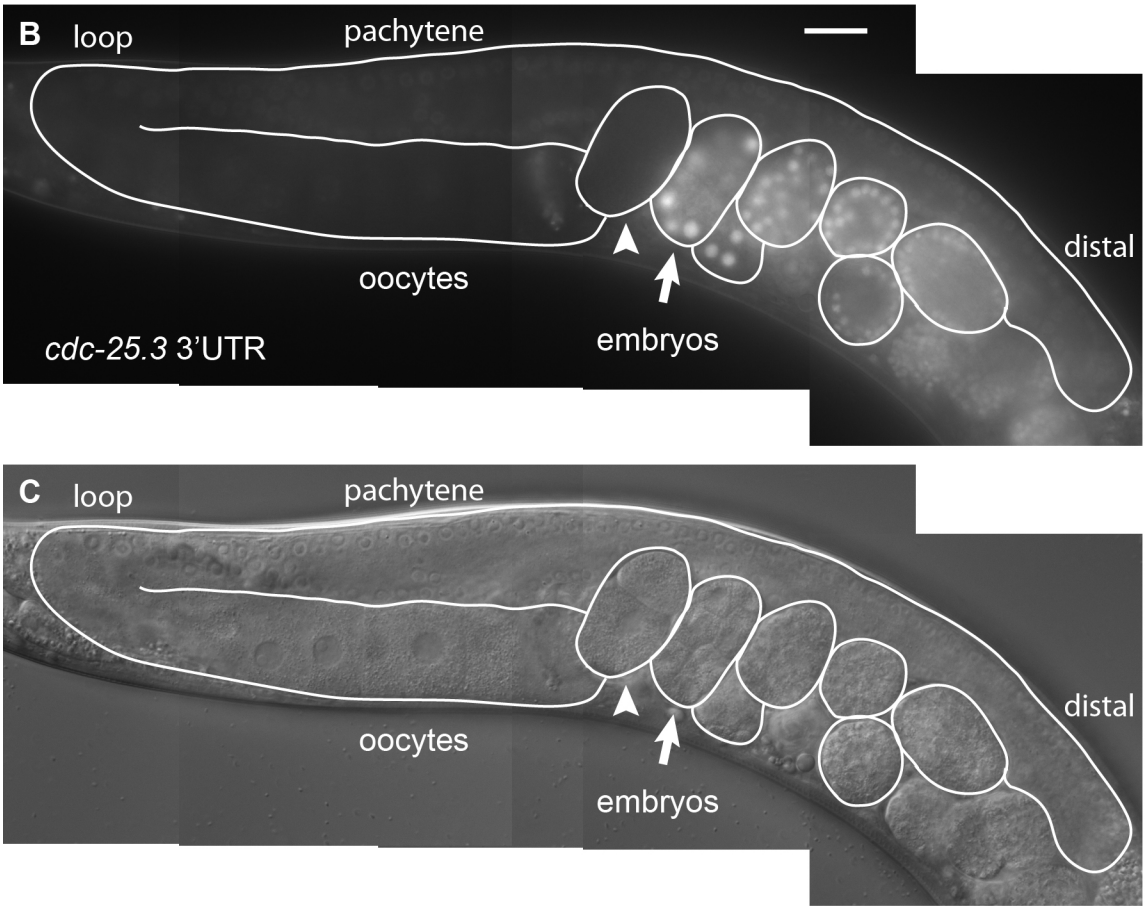

Figure S5 Different patterns of GFP::H2B expression from the 3'UTR reporter transgenes described in the text. (A) The relative brightness of GFP::H2B expression in the germ lines of animals expressing each 3'UTR construct. GFP::H2B was either judged to be absent (–), sometimes present but very low and difficult to see (+/–), always present (+), or always present and bright relative to the other stages of germ line development (++) for that particular construct. Brightness levels represented here cannot be compared between the different 3'UTR constructs. GFP::H2B expression during early embryogenesis indicates the general trend (e.g., present or absent) rather than the relative strength of expression. Constructs that are repressed by *oma-1*

and *oma-2* are highlighted. Strongly repressed constructs are in dark gray and weakly repressed constructs in light gray. (B, C) GFP::H2B expression (B) from the *cdc-25.3* 3'UTR reporter construct in an otherwise wild-type animal (C). The U-shaped gonad arm and embryos are outlined, and the relative positions of the regions described in (A) are indicated. GFP::H2B is not expressed in 2-cell embryos (arrowhead) but is strongly expressed in slightly older embryos (arrow). Note that the images shown in Figure 4 and Figure S4, which often include pachytene nuclei as well as oocytes, are oriented as shown here. Bar, 20 μm.

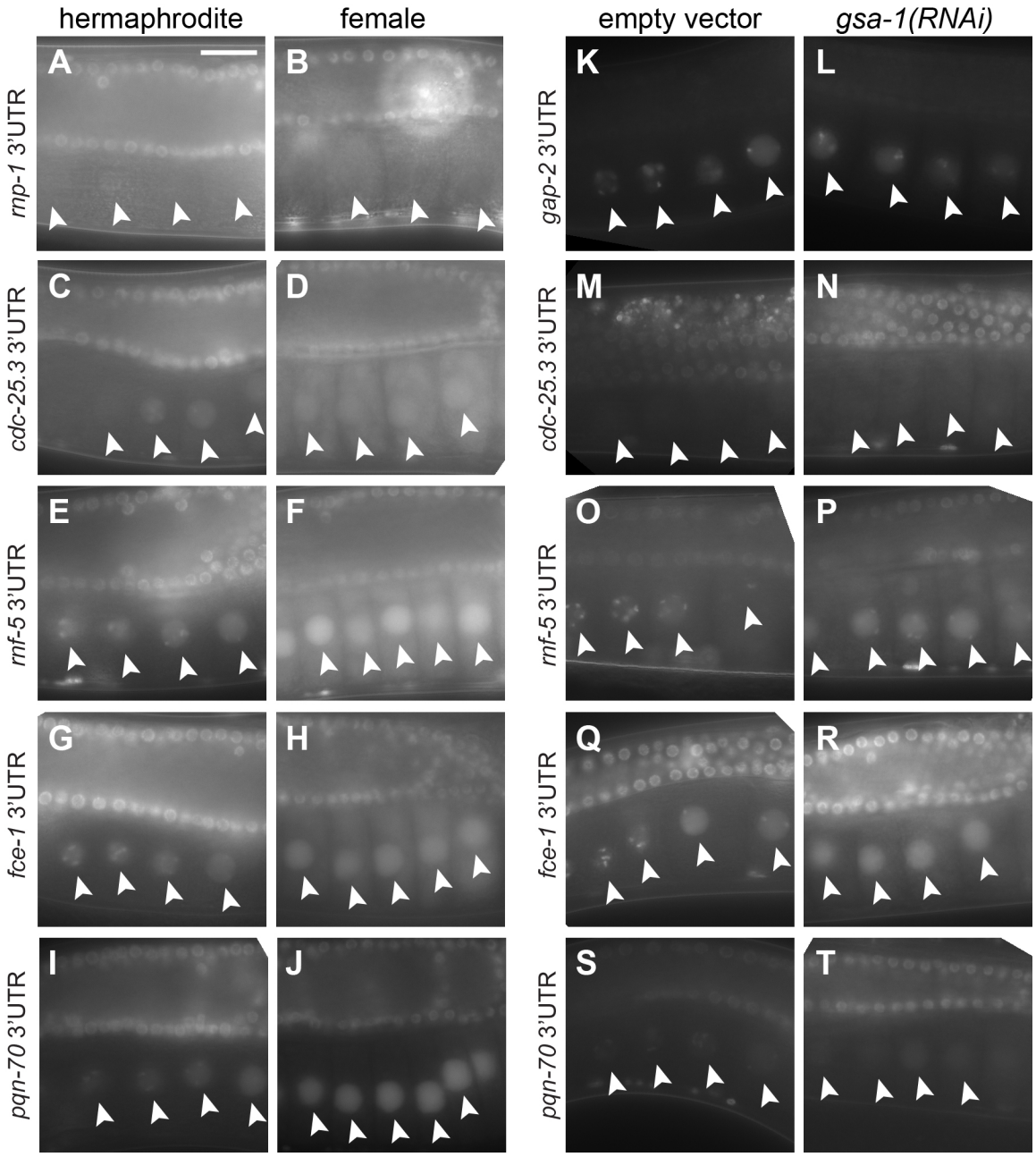

Figure S6 GFP::H2B expression from reporter transgenes is not dramatically altered in oocytes with a reduced rate of oocyte maturation. (A–J) The oocytes of *fog-2(oz40)* females (B, D, F, H, J) were compared to the oocytes of hermaphrodites (A, C, E, G, I). (K–T) The oocytes of *gsa-1(RNAi)* animals (L, N, P, R, T) were compared to the oocytes of animals exposed to a non-targeting RNAi construct (K, M, O, Q, S). All animals were homozygous for the indicated 3'UTR reporter transgene. Modest, but reproducible, increases in nuclear GFP expression were observed for the *rnf-5* and *pqn-70* 3'UTR constructs in female oocytes (F, J). Nuclear GFP expression levels of the *rnf-5* 3'UTR construct increased even further after *oma-1/2(RNAi)* in *fog-2* females (Figure S7). Expression of all 3'UTR constructs, including the *rnp-1* construct, which is not shown, appeared to be unaffected by *gsa-1(RNAi)* (D. Coetzee, unpublished results). Bar, 20 µm.

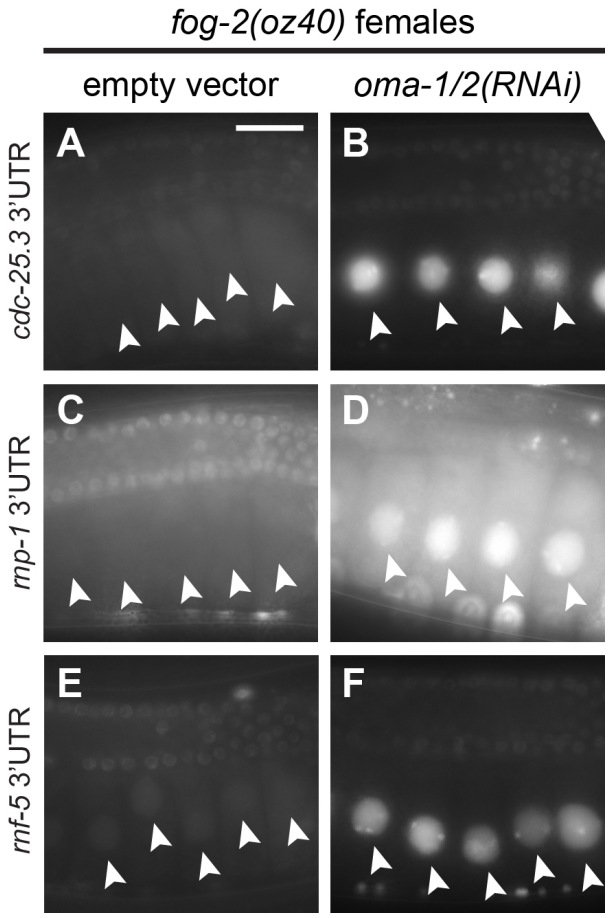

Figure S7 GFP::H2B expression from reporter transgenes is increased in *fog-2(oz40)* females after *oma-1/2(RNAi)*. (A–F) The oocytes of *fog-2(oz40)* animals exposed to *oma-1/2(RNAi)* (B, D, F) were compared to the oocytes of *fog-2(oz40)* animals exposed to a non-targeting RNAi construct (A, C, E). Bar, 20 µm.

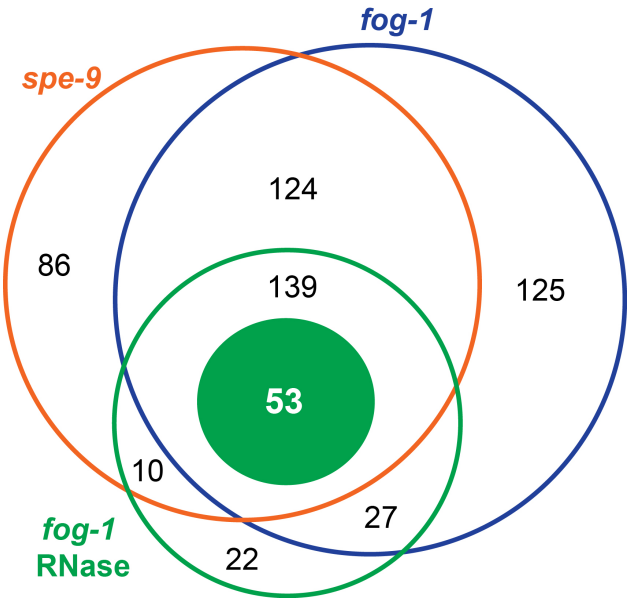

Figure S8 Overlapping sets of proteins were identified in OMA-1 purifications. Identified proteins, counted as NCBI GI numbers with at least two peptide matches, are illustrated for each sample. Purifications performed in the presence of RNA (orange and blue circles) identified more proteins than the RNAse-treated purification (empty green circle), with substantial overlap among all three samples. Proteins present in all three OMA-1 purifications, but absent from control purifications and not identified as abundant contaminants (see *Materials and Methods*), are candidates for proteins that interact with OMA-1 in oocytes (solid green circle). A few of the protein accession numbers appear to be redundant (e.g., GLD-2; see File S2). Such duplicates were removed from the numbers mentioned in the text. Because the yield of OMA RNPs appears greater when purifications are conducted from females as opposed to hermaphrodites, we did not conduct a large number of experimental replicates in an attempt to identify proteins that depend on the presence or absence of sperm for their association with OMA-1.

Table S1 *C. elegans* strains used for this study

Strain	Genotype
N2	Wild type, Bristol isolate
BS553	*fog-2(oz40)* V
TX174	*oma-1(zu405te33)* IV
TX431	*oma-2(te51)* V
DG2507	*oma-1(zu405te33)* IV*/nT1[qIs51]* (IV;V)*; oma-2(te51)* V*/nT1[qIs51]* (IV;V)
DG2531	*unc-119(ed3)* III*; oma-1(zu405te33)* IV*; tnIs17[pCS410 oma-1p::oma-1::s::tev::gfp, pDPMM0016B unc-119(+)]* V
DG2460	*spe-9(hc88*ts*)* I; *oma-1(zu405te33)* IV
DG2462	*fog-1(q253*ts*)* I; *oma-1(zu405te33)* IV
DG2566	*fog-1(q253*ts*)* I*; oma-1(zu405te33)* IV*; tnIs17[pCS410 oma-1p::oma-1::s::tev::gfp, pDPMM0016B unc-119(+)]* V
DG2581	*spe-9(hc88*ts*)* I*; oma-1(zu405te33)* IV*; tnIs17[pCS410 oma-1p::oma-1::s::tev::gfp, pDPMM0016B unc-119(+)]* V
DG2620	*unc-119(ed3)* III*; oma-1(zu405te33)* IV*; oma-2(te51) tnIs17[pCS410 oma-1p::oma-1::s::tev::gfp, pDPMM0016B unc-119(+)]* V
DG2632	*acy-4(ok1806) tnIs17[pCS410 oma-1p::oma-1::s::tev::gfp, pDPMM0016B unc-119(+)]* V*/nT1[qIs51]* (IV;V)
DG2713	*fog-2(q71)* V*; teIs1[pRL475 oma-1p::oma-1::GFP, pDPMM016 unc-119(+)]*
DG3212	*unc-119(ed3)* III*; tnIs36[pCS450 pie-1p::gfp::h2b::cdc-25.3 3'UTR, unc-119(+)]*
DG3228	*unc-119(ed3)* III*; tnIs48[pCS450 pie-1p::gfp::h2b::cdc-25.3 3'UTR, unc-119(+)]*
DG3238	*unc-119(ed3)* III*; tnIs53[pCS456 pie-1p::gfp::h2b::rnf-5 3'UTR, unc-119(+)]*
DG3239	*unc-119(ed3)* III*; tnIs54[pCS456 pie-1p::gfp::h2b::rnf-5 3'UTR, unc-119(+)]*
DG3242	*unc-119(ed3)* III*; tnIs57[pCS458 pie-1p::gfp::h2b::rnp-1 3'UTR, unc-119(+)]*
DG3262	*unc-119(ed3)* III*; tnIs64[pCS464 pie-1p::gfp::h2b::fce-1 3'UTR, unc-119(+)]*
DG3275	*unc-119(ed3)* III*; tnIs77[pCS466 pie-1p::gfp::h2b::pqn-70 3'UTR, unc-119(+)]*
DG3278	*unc-119(ed3)* III*; tnIs80[pCS468 pie-1p::gfp::h2b::wdr-23 3'UTR, unc-119(+)]*
DG3300	*unc-119(ed3)* III*; tnIs87[pDC5 pie-1p::gfp::h2b::rom-1 3'UTR, unc-119(+)]*
DG3309	*unc-119(ed3)* III*; tnIs93[pDC22 pie-1p::gfp::h2b::gap-2 3'UTR, unc-119(+)]*
DG3328	*unc-119(ed3)* III*; tnIs95[pDC18 pie-1p::gfp::h2b::fbf-2 3'UTR, unc-119(+)]*
DG3333	*unc-119(ed3)* III*; oma-2(te51)* V*; tnIs64[pCS464 pie-1p::gfp::h2b::fce-1 3'UTR, unc-119(+)]*
DG3336	*unc-119(ed3)* III*; oma-2(te51)* V*; tnIs57[pCS458 pie-1p::gfp::h2b::rnp-1 3'UTR, unc-119(+)]*
DG3359	*unc-119(ed3)* III*; oma-1(zu405te33)* IV*; tnIs36[pCS450 pie-1p::gfp::h2b::cdc-25.3 3'UTR, unc-119(+)]*
DG3385	*unc-119(ed3)* III*; oma-2(te51)* V*; tnIs77[pCS466 pie-1p::gfp::h2b::pqn-70 3'UTR, unc-119(+)]*
DG3600	*unc-119(ed3)* III*; oma-1(zu405te33)* IV*/nT1[qIs51]* (IV;V)*; oma-2(te51) V/nT1[qIs51]* (IV;V)*; tnIs53[pCS456 pie-1p::gfp::h2b::rnf-5 3'UTR, unc-119(+)]*
TX1248	*unc-119(ed3) teIs114[pRL2701 pie-1p::gfp::h2b::zif-1 3'UTR, unc-119(+)]* III
DG3246	*fog-2(oz40)/+* V*; tnIs57[pCS458 pie-1p::gfp::h2b::rnp-1 3'UTR, unc-119(+)]*
DG3261	*fog-2(oz40)/+* V*; tnIs36[pCS450 pie-1p::gfp::h2b::cdc-25.3 3'UTR, unc-119(+)]*
DG3284	*fog-2(oz40)/+* V*; tnIs64[pCS464 pie-1p::gfp::h2b::fce-1 3'UTR, unc-119(+)]*
DG3285	*fog-2(oz40)/+* V*; tnIs54[pCS456 pie-1p::gfp::h2b::rnf-5 3'UTR, unc-119(+)]*

Table S1 (continued) *C. elegans* strains used for this study

Strain	Genotype
DG3286	*fog-2(oz40)/+* V*; tnIs53[pCS45 (pie-1p::gfp::h2b::rnf-5 3'UTR, unc-119(+)]*
DG3302	*fog-2(oz40)/+* V*; tnIs77[pCS466 pie-1p::gfp::h2b::pqn-70 3'UTR, unc-119(+)]*
DG3306	*fog-2(oz40)/+* V*; tnIs48[pCS450 pie-1p::gfp::h2b::cdc-25.3 3'UTR, unc-119(+)]*
DG3338	*rnp-1(ok1549)* V*/nT1[qIs51]* (IV;V)
DG3371	*fog-3(q470) unc-13(e1091)/++* I*; rnp-1(ok1549)*V*/nT1[qIs51]* (IV;V)
DG3155	*cdc-25.3(ok358)* III
DG3502	*lin-41(ma104)* I*; unc-119(ed3) teIs114[pRL2701 pie-1p::gfp::h2b::zif-1 3'UTR, unc-119(+)]* III
DG3501	*lin-41(ma104)* I
DG3786	*lin-41(tn1487*ts*)* I*/hT2* (I;III)*; unc-119(ed3)* III*/ hT2[bli-4(e937) let-?(q782) qIs48]* (I;III)*; tnIs36[pCS450 pie-1p::gfp::h2b::cdc-25.3 3'UTR, unc-119(+)]*
DG3792	*lin-41(tn1487*ts*)*I*; unc-119(ed3) teIs114[pRL2701 pie-1p::gfp::h2b::zif-1 3'UTR, unc-119(+)]* III
DG2882	*lin-41(n2914)* I*/hT2* (I;III)*; unc-119(ed3) teIs114[pRL2701 pie-1p::gfp::h2b::zif-1 3'UTR, unc-119(+)]* III */hT2[bli-4(e937) let-?(q782) qIs48]* (I;III)

Table S2 Relative quantification of *zif-1* and *nos-2* target mRNA levels in OMA-1 purifications (IPs) using RT-PCR and RNA sequencing

	RT-PCR		RNAseq
	spe-9 IPs (Mean ± SD)	*fog-1* IPs (Mean ± SD)	*fog-1* IP4
zif-1/nos-2 mRNA	5.7 ± 2.1	5.6 ± 1.7	5.1

Files S1 and S2

Available for download at http://www.genetics.org/lookup/suppl/doi:10.1534/genetics.114.168823/-/DC1.

File S1 Identification and analysis of OMA-1-associated mRNAs.

File S2 Identification and analysis of OMA-1-associated proteins.